Journal of Catalysis 287 (2012) 1–4

Contents lists available at SciVerse ScienceDirect

Journal of Catalysis

journal homepage: www.elsevier.com/locate/jcat

Priority Communication

Thermal and catalytic formation of radicals during autoxidation

Ulrich Neuenschwander, Ive Hermans *

Institute for Chemical and Bioengineering, Department of Chemistry and Applied Biosciences, ETH Zurich, Wolfgang-Pauli-Strasse 10, CH-8093 Zurich, Switzerland

ARTICLE INFO

Article history:
Received 19 September 2011
Revised 29 November 2011
Accepted 8 December 2011
Available online 12 January 2012

Keywords:
Kinetics
Initiation
Oxidation
Radicals
Mechanism

ABSTRACT

The aerobic autoxidation of hydrocarbons proceeds through a complicated reaction mechanism, mediated by free radicals. Most reported autoxidation catalysts enhance the radical formation rate *via* homolytic activation of hydroperoxide products. Whereas our knowledge of the product formation mechanisms has significantly improved over the last couple of years, the chain-initiation is still poorly understood. In this contribution, the thermal and catalytic initiation rate for the oxidation of the renewable olefin α-pinene is quantified, thereby providing evidence for a substrate-assisted thermal initiation. The kinetics of the catalytic initiation is in good agreement with previous studies under model conditions.

1. Introduction

Partial oxidation of hydrocarbons is an industrially relevant and academically challenging task [1]. One important class of aerobic oxidations are autoxidations, mediated by free radical intermediates [2–4]. Important bulk scale processes which are based on this chemistry are, for example, the oxidation of *p*-xylene to terephthalic acid (44×10^6 tons per year), the oxidation of cyclohexane to cyclohexanol and cyclohexanone (6×10^6 tons per year), and the synthesis of ethylbenzene hydroperoxide (6×10^6 tons per year) [3]. When a hydrocarbon (RH) is subjected to oxygen at elevated temperatures, a chain oxidation takes place during which the active oxidant is not O_2 itself, but reactive peroxyl radicals (ROO·) [4]. Products which can be observed are hydroperoxides (ROOH), alcohols (ROH), and ketones (Q=O). Under non-catalytic conditions, radicals are generated from the ROOH product, leading to an autocatalytic increase in the oxidation rate [4]. Although it had been assumed [3] that this thermal chain-initiation takes place *via* homolytic dissociation of the O—O bond (reaction (1)), it was recently proposed that this unimolecular reaction is not only very slow, but also inefficient in generating radicals, as the nascent radical-pair rapidly recombines in a solvent-cage [5]. It was therefore proposed that the initiation is a bimolecular reaction between ROOH and the substrate (reaction (2)), or a more reactive reaction product, such as cyclohexanone in the case of cyclohexane oxidation (reaction (3)). In those reactions, the OH-radical breaking away from the hydroperoxide abstracts an H-atom, forming water and a C-centered radical, eventually stabilized by delocalization [5]. Such a substrate or product-induced initiation not only features a lower activation barrier, it is also proposed to be more efficient in generating radicals than the unimolecular O—O bond cleavage, because the nascent RO·-radical is effectively shielded by the initially hydrogen-bonded water molecule against recombination with the R·-radical[1].

$$\mathrm{ROOH} \rightarrow \mathrm{RO^{\cdot}} + {\cdot}\mathrm{OH} \quad (1)$$

$$\mathrm{ROOH} + \mathrm{RH} \rightarrow \mathrm{RO^{\cdot}} + \mathrm{H_2O} + \mathrm{R^{\cdot}} \quad (2)$$

$$\mathrm{ROOH} + \mathrm{Q{=}O} \rightarrow \mathrm{RO^{\cdot}} + \mathrm{H_2O} + \mathrm{Q_{-\alpha H^{\cdot}}{=}O} \quad (3)$$

The RO· radicals are rapidly converted to R· radicals (reaction (4)) which are themselves trapped by O_2, leading to ROO· radicals (reaction (5)). Peroxyl radicals are able to abstract H-atoms from the substrate and form ROOH (reaction (6)).

$$\mathrm{RO^{\cdot}} + \mathrm{RH} \rightarrow \mathrm{ROH} + \mathrm{R^{\cdot}} \quad (4)$$

$$\mathrm{R^{\cdot}} + \mathrm{O_2} \rightarrow \mathrm{ROO^{\cdot}} \quad (5)$$

$$\mathrm{ROO^{\cdot}} + \mathrm{RH} \rightarrow \mathrm{ROOH} + \mathrm{R^{\cdot}} \quad (6)$$

In addition, ROO· radicals can abstract the weakly bonded α H-atom of the ROOH primary product, leading to the formation of alcohol and ketone in an activated solvent-cage reaction (7); the stoichiometric coefficient *x* in reaction (7) depends on the substrate [6–9].

* Corresponding author. Fax: +41 44 6331514.
E-mail address: hermans@chem.ethz.ch (I. Hermans).

[1] H_2O acts as "insulator" between the two radicals and is hydrogen-bonded to the alkoxyl radical with approximately 2.6 kcal mol^{-1}, at the ZPE-corrected UB3LYP/6-311++G(df,pd) level of theory.

0021-9517/$ - see front matter © 2011 Elsevier Inc. All rights reserved.
doi:10.1016/j.jcat.2011.12.009

$$ROO^{\cdot} + ROOH\{+RH\} \rightarrow xROOH + xR^{\cdot} + (1-x)ROH + (1-x)RO^{\cdot} + Q{=}O + H_2O \quad (7)$$

Reactions (8) and (9) can be additional sources of alcohol and ketone, respectively, depending on the substrate [10].

$$RO^{\cdot} + ROOH \rightarrow ROH + ROO^{\cdot} \quad (8)$$

$$RO^{\cdot} + O_2 \rightarrow Q{=}O + HO_2 \quad (9)$$

As compared to saturated hydrocarbons, olefins are significantly more reactive. Among other reasons, this is caused by a better stabilization of the electron-deficient R· radicals (allylic resonance). Moreover, the ROO· radicals can, in addition to H-abstraction, add to the C=C bond, forming epoxide (EO) (reaction (10)) [10]. The efficiency of this epoxidation mechanism depends on the olefin as well as the O_2 partial pressure [11,12].

$$ROO^{\cdot} + RH \rightarrow RO^{\cdot} + EO \quad (10)$$

In all cases, one also has to consider the cross-reaction of ROO· radicals, despite the low [ROO·] ($\approx 10^{-7}$ M); this reaction can either lead to alkoxyl radicals (reaction (11)) or chain-termination (reaction (12)). The substrate-dependent branching ratio between the two channels has important consequences on the whole chain mechanism [13].

$$ROO^{\cdot} + ROO^{\cdot} \rightarrow RO^{\cdot} + RO^{\cdot} + O_2 \quad (11)$$

$$ROO^{\cdot} + ROO^{\cdot} \rightarrow ROH + Q{=}O + O_2 \quad (12)$$

Most reported autoxidation catalysts accelerate the formation of radicals by homolytic activation of hydroperoxides [2]. The best known catalysts are based on $Co^{II/III}$, accelerating the decomposition of the hydroperoxide in a so-called Haber–Weiss cycle (reactions (13) and (14)) [14]. The catalyst can be homogeneous (industrial practice) or heterogeneous, for example, incorporated in a (micro-) porous material [15].

$$ROOH + Co^{II} \rightarrow Co^{III}{-}OH + RO^{\cdot} \quad (13)$$

$$ROOH + Co^{III}{-}OH \rightarrow Co^{II} + H_2O + ROO^{\cdot} \quad (14)$$

The rate of this reaction has been directly measured for the model hydroperoxide *t*-BuOOH and $Co^{II}(acac)_2$, dissolved in cyclohexane using *in situ* UV–Vis spectroscopy [16]. In the temperature range 323–343 K, the rate constant can be well represented by the Arrhenius expression $k_{cat}(T) = (6 \pm 3) \times 10^8\ M^{-1}\ s^{-1} \times \exp(-13 \pm 2\ kcal\ mol^{-1}/RT)$.

However, up until now, there is no direct *in situ* quantification of the catalytic initiation rate constant under autoxidation conditions. Neither is there a quantification of the relative importance of the catalytic initiation to the total initiation. A better understanding of catalytic autoxidation chemistry should start with a kinetic quantification of the catalyst's performance.

2. Materials and methods

The experiments were performed in a 10-mL glass bubble column reactor equipped with a top condenser. O_2 was bubbled (100 N mL/min) through 250 μm pores of a bubbler to ensure fast gas–liquid mass-transfer. The mixing of the liquid by the gas bubbles was adequate: Tests with dye solutions revealed a mixing time of about 2–3 s. The temperature was controlled by a thermostat, equipped with an immersion heater and thermocouple. The reactor was heated to reaction temperature under a flow of N_2 (inert conditions); subsequently, the gas flow was changed to O_2 to start the reaction. It should be noted that this is potentially dangerous and that appropriate safety measures should be taken; for instance, working at low scales and ensuring an excess of O_2 in the gas phase to stay above the explosion limit. *n*-Nonane (Sigma Aldrich, >99 %) was added in 1 mol% as an internal standard to freshly distilled α-pinene (98%, Sigma–Aldrich, stabilized). The distilled substrate had a GC purity of about 99%, was phenol-stabilizer free, and the main impurity was the substrate isomer β-pinene. Product quantification was done with GC–FID and GC–MS, as described elsewhere [10]. In agreement with an earlier study by some of us [17], the effect of the glass wall on this oxidation reaction was negligible.

3. Results and discussion

As a benchmark reaction for characterizing the catalytic activity of $Co(acac)_2$, a well-known autoxidation model-catalyst, we chose the autoxidation of the renewable olefin α-pinene. The most prominent products during α-pinene oxidation are α-pinene oxide, verbenyl hydroperoxide, verbenol, and verbenone (Scheme 1), whereas other regioisomeric products have also been characterized [10]. Most of these products are interesting targets for the fragrance and flavor industry, for example, the epoxide is the starting material for the synthesis of sandalore® (Givaudan) and polysantol® (Firmenich) [18].

It is known from our earlier work that the oxidation rate is directly linked to the concentration of chain-carrying peroxyl radicals [10]. Fig. 1 shows that upon addition of 100 μM catalyst, the oxidation rate is significantly enhanced. Addition of 500 mM verbenol did not affect the reaction rate, showing that reaction products barely influenced the catalytic activity.

In order to quantify the catalytic effect, a series of experiments with varying catalyst concentration was performed. The observed rates increased as a function of the $Co(acac)_2$ concentration, but in a nonlinear way, implying an indirect connection of the catalyst concentration with the reaction rate. During autoxidations, the radical's lifetime is significantly shorter than the timescale of the overall oxidation reaction, leading to radical quasi steady-state [5]. The rate of chain-initiation therefore equals the rate of chain-termination (Eq. (A)), allowing for an evaluation of the instantaneous radical concentration (Eq. (B)).

$$k_2[ROOH][RH] + k_{cat}[ROOH][Co^{II}] \equiv k_{12}[ROO^{\cdot}]^2 \quad (A)$$

$$[ROO^{\cdot}] = \sqrt{\frac{k_2[ROOH][RH] + k_{cat}[ROOH][CO^{II}]}{k_{12}}} \quad (B)$$

It should be noted that there is a thermal contribution (k_2[ROOH][RH]) and a catalytic contribution (k_{cat}[ROOH][Co^{II}]) to the initiation; k_{cat} refers to the rate constant of the rate-determining step in the Haber–Weiss cycle.[2] The propagation rate (r_p) is proportional to [ROO·] and [RH] (Eq. (C)), with k_p referring to the propagation rate constant, *i.e.* the sum of H-abstraction and C=C addition in case of α-pinene [10]. Therefore, an elegant way to linearize the equations – and to determine k_{cat} – is to plot the squared-rate at a given [ROOH] *vs.* the catalyst concentration. The slope (Eq. (E)) of this squared-rate plot is a measure for the Haber–Weiss reactivity of the catalyst, whereas the intercept (Eq. (F)) contains information about the pure thermal initiation.

$$r_p = k_p[ROO^{\cdot}][RH] \quad (C)$$

$$r_p^2 = \text{intercept} + \text{slope} \times [CO^{II}] \quad (D)$$

$$\text{Slope} = \frac{k_{cat} \times k_p^2}{k_{12}}[RH]^2[ROOH] \quad (E)$$

[2] That the concentration of the active catalyst species involved in the rate-determining step is present in a concentration which is nearly the same as the initially added $[Co(acac)_2]_0$.

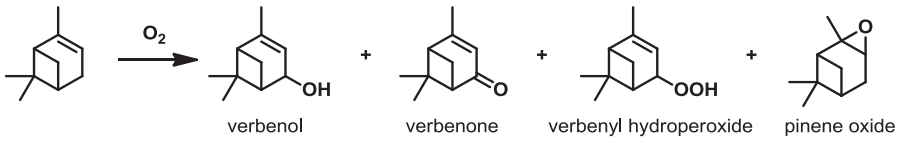

Scheme 1. Main products of the thermal α-pinene oxidation.

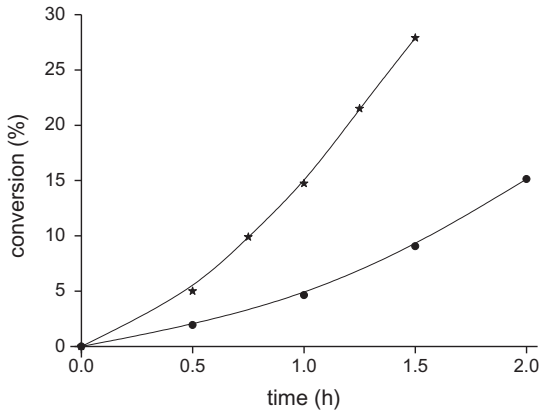

Fig. 1. The time-evolution of the sum of products under thermal (•) and catalytic conditions (★, 100 μM $Co(acac)_2$), both at 353 K (1 atm O_2).

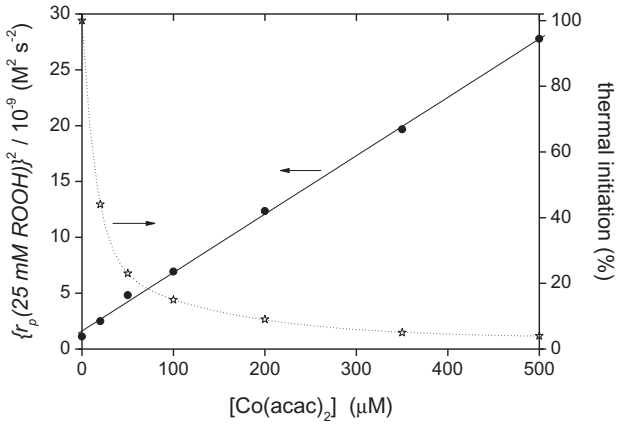

Fig. 3. Squared-rate plot of $Co(acac)_2$ catalyzed α-pinene autoxidation (•, solid line) at 353 K and [ROOH] = 25 mM; intercept = 1.6×10^{-9} M^{-1} s^{-1}; slope = 5.3×10^{-5} M^{-1} s^{-1}. Contribution of thermal initiation (☆, dotted line).

$$\text{Intercept} = \frac{k_2 k_p^2}{k_{12}}[\text{RH}]^3[\text{ROOH}] \qquad \text{(F)}$$

The slope of $\sum_i[\text{Product}_i]$ *vs.* time was determined for every experimental data point and plotted as a function of the experimentally measured [ROOH] (see Fig. 2); this procedure was repeated for various concentrations of $Co(acac)_2$. The obtained r_p(25 mM ROOH) data were used to construct the squared-rate *vs.* [$Co(acac)_2$] plot in Fig. 3. Repetition experiments showed that the combined experimental and analytical error is about 10% for each data point. The validity of the linear model over a large catalyst concentration range corroborates the presence of a thermal and catalytic term in the initiation mechanism. Applying the kinetic expressions (A)–(F), a quantitative data evaluation can be done. The extracted k_{cat} = 0.5 M^{-1} s^{-1} at 353 K is approximately ten times smaller than the value measured for *t*-BuOOH in cyclohexane under model conditions. This difference in reactivity might be related to the different steric requirements of pinene hydroperoxide *vs.* *t*-BuOOH. The observed k_{cat}/k_2 ratio is $\approx 3 \times 10^5$, showing that the Haber–Weiss initiation is orders of magnitude faster than thermal initiation. Therefore, already at a catalyst concentration of only 3 ppm (*i.e.*, 20 μM), the initiation caused by the catalyst (reactions (11) and (12)) outruns the thermal "self-initiation" of hydroperoxide (reaction (2)).

In order to obtain more kinetic data, series of autoxidation experiments were carried out at different temperatures. The resulting rate-square plots are shown in Fig. 4. It should be noted that under the chosen conditions, gas/liquid mass-transfer cannot be limiting, since the rate can be accelerated with cobalt catalyst, still staying at a constant oxygen supply.

From the slope and intercept of these plots, and the known k_p and k_{12} [10], one can determine $k_{cat}(T) = (3 \pm 2) \times 10^8 \times \exp(-14 \pm 2 \text{ kcal mol}^{-1}/RT)$ and $k_2(T) = (5 \pm 2) \times 10^8 \times \exp(-23 \pm 2 \text{ kcal mol}^{-1}/RT)$. These results show that the activation barrier of the thermal initiation mechanism is substantially lower than the RO—OH bond dissociation energy (*viz.* 23 *vs.* 40 kcal mol^{-1}) but in good agreement with the UB3LYP/6-311++G(df,pd)//UB3LYP/6-31G(d,p) predicated barrier of reaction (2), *i.e.*, 24.5 kcal mol^{-1}. To the best of our

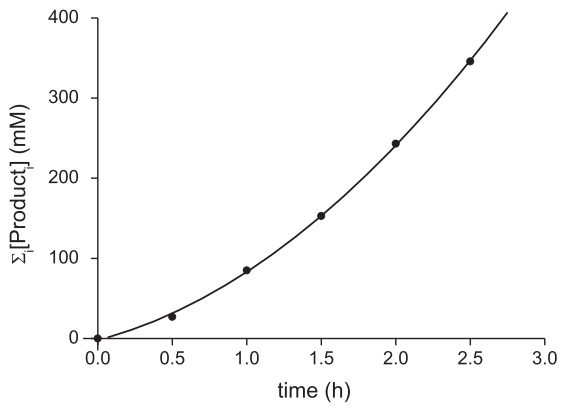

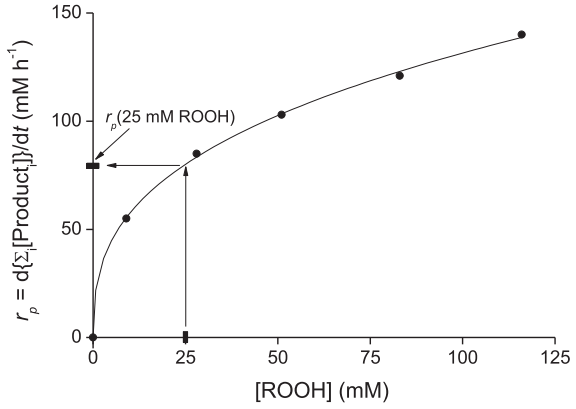

Fig. 2. Procedure to determine r_p (25 mM ROOH): left-hand of the figure shows $\sum_i[\text{Product}_i]$ *vs.* time for 50 μM $Co(acac)_2$ at 343 K; right-hand of the figure shows $r_p = d\{\sum_i[\text{Product}_i]\}/dt$ as a function of [ROOH]. r_p (25 mM ROOH) can be found *via* interpolation.

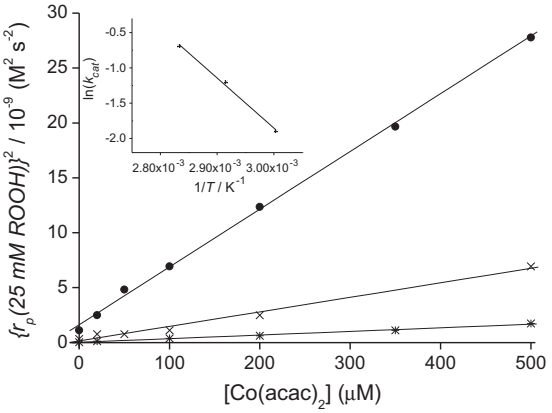

Fig. 4. Squared-rate at 25 mM ROOH *vs.* [$Co(acac)_2$] for α-pinene autoxidation at 353 K (•), 343 K (×) and 333 K (*). The insert shows the Arrhenius plot for k_{cat} as determined from the slope of the plots (see text).

knowledge, this is the first direct experimental evidence for the proposed bimolecular initiation mechanism (reaction (2)). It should be noted that a rigorous falsification of the unimolecular initiation (reaction (1)) can be done: Whereas the intercept (Eq. (F)) would be dependent on $[RH]^2$ instead of $[RH]^3$ – *i.e.*, k_1 would be a factor of [RH] higher than k_2 – the temperature-dependence would still be the same for both approaches, hence in disagreement with the involved unimolecular activation energy. The Arrhenius expression for k_{cat} is found in good agreement with the one derived under model conditions with *in situ* UV–Vis spectroscopy (*i.e.*, using *t*BuOOH in cyclohexane [16]), *viz.* $(6 \pm 3) \times 10^8 \times \exp(-13 \pm 2 \text{ kcal mol}^{-1}/RT)\text{M}^{-1}\text{ s}^{-1}$, and underlines the robustness of our analysis[3]. An analogous data evaluation procedure can be used to study the performance of other oxidation catalysts, including heterogeneous catalytic systems.

4. Conclusions

In this contribution, we determined the Arrhenius expressions for the temperature-dependence of the rate constants for thermal and $Co(acac)_2$-catalyzed chain-initiation during the autoxidation of α-pinene. The kinetic analysis is based on a quasi steady-state treatment of the chain-carrying peroxyl radicals and allows for a precise determination of the rate constants under reaction conditions. It is shown that the activation energy of the thermal chain-initiation (*viz.* $23 \pm 2 \text{ kcal mol}^{-1}$) is significantly lower than the RO—OH bond strength (40 kcal mol^{-1}), ruling out a unimolecular homolytic cleavage. However, the experimentally determined activation energy is in good agreement with the DFT-predicted barrier (*i.e.* $24.5 \text{ kcal mol}^{-1}$) of a substrate-assisted initiation mechanism in which the OH-radical breaking away from the RO—OH abstracts a weakly bonded allylic H-atom from α-pinene. The rate constant of the rate-determining step of the catalytic chain-initiation mechanism is in quantitative agreement with previously determined kinetic data on the deperoxidation of *t*BuOOH using *in situ* UV–Vis spectroscopy. Starting at a $Co(acac)_2$ concentration of 20 μM onwards, the catalytic chain-initiation dominates over the thermal substrate-assisted initiation mechanism. The approach of obtaining (catalytic) kinetic data from plotting squared-rates at constant ROOH concentrations – as reported in this work – can analogously be applied to other important oxidation reactions, for example, the oxidation of *p*-xylene to terephthalic acid or cyclohexane to K/A-oil.

Acknowledgments

Financial support of the ETH Zurich and the Swiss National Science Foundation (SNSF) is kindly acknowledged by the authors.

References

[1] F. Cavani, J.H. Teles, ChemSusChem 2 (2009) 508–534.
[2] R.A. Sheldon, J.K. Kochi, in: Metal-Catalyzed Oxidations of Organic Compounds, Academic Press, New York, 1981.
[3] G. Franz, R.A. Sheldon, in: Oxidation, Ullmann's Encyclopedia of Industrial Chemistry, Wiley-VCH, Weinheim, 2000.
[4] N.M. Emanuel, E.T. Denisov, Z.K. Maizus, in: Liquid Phase Oxidation of Hydrocarbons, Plenum, New York, 1967.
[5] I. Hermans, P.A. Jacobs, J. Peeters, Chem. Eur. J. 12 (2006) 4229–4240.
[6] I. Hermans, T.L. Nguyen, P.A. Jacobs, J. Peeters, ChemPhysChem 6 (2005) 637–645.
[7] I. Hermans, J. Peeters, P.A. Jacobs, J. Org. Chem. 72 (2007) 3057–3064.
[8] I. Hermans, P.A. Jacobs, J. Peeters, J. Mol. Catal. A 251 (2006) 221–228.
[9] I. Hermans, J. Peeters, L. Vereecken, P. Jacobs, ChemPhysChem 8 (2007) 2678–2688.
[10] U. Neuenschwander, F. Guignard, I. Hermans, ChemSusChem 3 (2010) 75–84.
[11] D.E. van Sickle, F.R. Mayo, J. Arluck, J. Am. Chem. Soc. 81 (1965) 4824–4832.
[12] U. Neuenschwander, I. Hermans, Phys. Chem. Chem. Phys. 12 (2010) 10542–10549.
[13] U. Neuenschwander, E. Meier, I. Hermans, ChemSusChem 4 (2011) 1621–1631.
[14] (a) F. Haber, J. Weiss, Naturwissenschaften 20 (1932) 948–950;
(b) F. Haber, J. Weiss, Proc. Roy. Soc. London Ser. A 147 (1934) 332–351;
(c) G. Sosnovsky, D.J. Rawlinson, in: D. Swern (Ed.), Organic Peroxides, vol. 2, Wiley, New York, 1971, p. 153;
(d) R.A. Sheldon, J.K. Kochi, Adv. Catal. 25 (1976) 272–413;
(e) S. Goldstein, D. Meyerstein, Acc. Chem. Res. 32 (1999) 547–550;
(f) W.H. Koppenol, Redox Rep. 6 (2001) 229–234.
[15] (a) See, for example F.X. Llabrés i. Xamena, O. Casanova, R.G. Tailleur, H. Garcia, A. Corma, J. Catal. 255 (2008) 220–227;
(b) D.L. Vanoppen, D.E. De Vos, M.J. Genet, P.G. Rouxhet, P.A. Jacobs, Angew. Chem. Int. Ed. 34 (1995) 560–563;
(c) A. Chica, G. Gatti, B. Moden, L. Marchese, E. Iglesia, Chem. Eur. J. 12 (2006) 1960–1967;
(d) K. Kervinen, H. Korpi, J.G. Mesu, F. Soulimani, T. Repo, B. Rieger, M. Leskelä, B.M. Weckhuysen, Eur. J. Inorg. Chem. (2005) 2591–2599.
[16] N. Turrà, U. Neuenschwander, A. Baiker, J. Peeters, I. Hermans, Chem. Eur. J. 16 (2010) 13226–13235.
[17] N. Turrà, A.B. Acuña, B. Schimmöller, B. Mayr-Schmölzer, P. Mania, I. Hermans, Top. Catal. 54 (2011) 737–745.
[18] K.G. Fahlbusch, F.J. Hammerschmitdt, J. Panten, W. Pickenhaben, D. Schatkowski, Flavors and Fragrances, Ullmann's Encyclopedia of Industrial Chemistry, Wiley-VCH, Weinheim, 2005.
[19] P.D. Lightfoot, R.A. Cox, J.N. Crowley, M. Destriau, G.D. Hayman, M.E. Jenkin, G.K. Moortgat, F. Zabel, Atmos. Environ. 27A (1992) 1805–1961.

[3] Due to the slight negative temperature dependence of the chain-length, i.e. -2 kcal /mol, [19] the observed activation energy of initiation is about 2 kcal/mol lower than the actual "true" value.